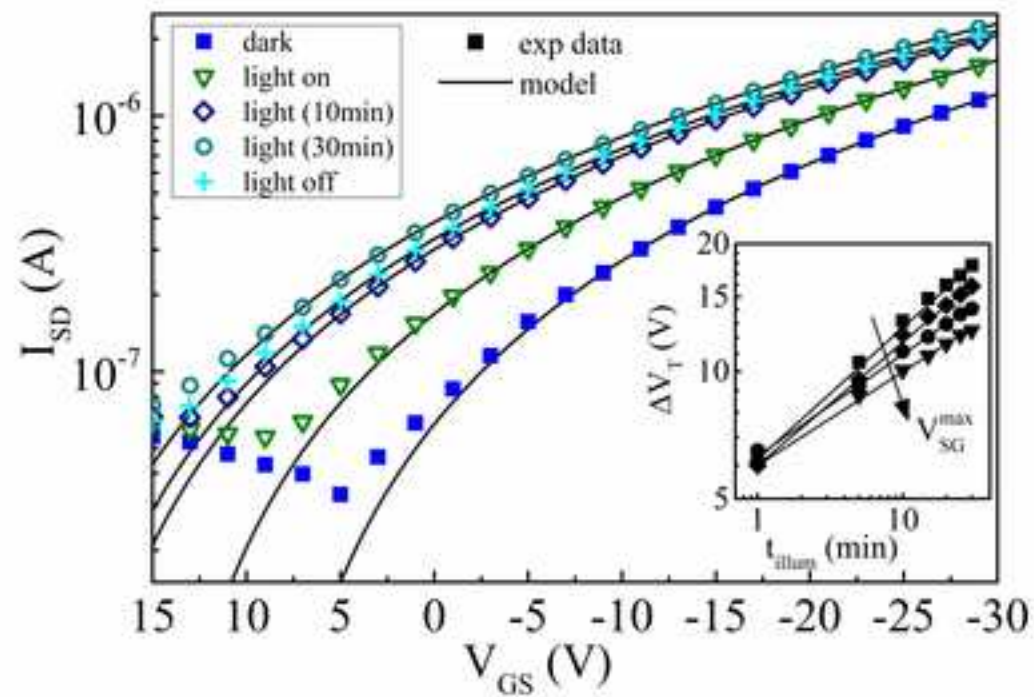
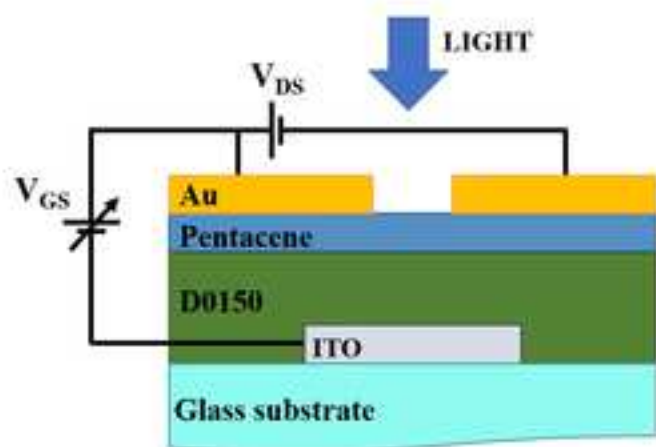


Light- and bias-induced effects in pentacene-based thin film phototransistors with a photocurable polymer dielectric

HIGHLIGHTS

- The prolonged and combined action of light and bias on pentacene OPTs is analyzed.
- Equations modeling organic phototransistor behavior are developed.
- Information about photon dose and gate bias during illumination is fundamental.
- Long-lived traps at insulator-OSC interface cause threshold voltage instability.
- Gate-bias stress effect can modulate the photosensitivity of organic devices.



Light- and bias-induced effects in pentacene-based thin film phototransistors with a photocurable polymer dielectric

R. Liguori^a, W. C. Sheets^b, A. Facchetti^{b,c}, and A. Rubino^a

^a*Department of Industrial Engineering (DIIn), University of Salerno, via Giovanni Paolo II, 132, 84084 Fisciano (SA), Italy*

^b*Polyera Corporation, 8045 Lamon Avenue, Skokie, IL, United States*

^c*Department of Chemistry and the Materials Research Center, Northwestern University, 2145 Sheridan Road, Evanston, IL, United States*

In this work, pentacene-based thin film phototransistors were fabricated with a photocurable polymer insulator and their electrical stability was monitored when the devices were exposed to light sources at different wavelengths. The magnitude of the photocurrent induced by illumination was found to be the result of two distinct factors: a direct photocurrent, related to electron-hole pair generation, and a current enhancement caused by a threshold voltage shift. The direction of threshold translation is attributed to the nature of trap states, specifically those located in the pentacene film near the interface with the polymer, and is affected by a measurement-induced effect, so that the photosensitivity can be modulated by a persistent gate bias during illumination. The equations for these two contributions were developed to study the light effects on material structure, the trapping process of electrons at the insulator-semiconductor interface and the photoconductive efficiency in the organic semiconductor.

1. INTRODUCTION

Organic thin film transistors (OTFTs) have gained considerable importance in recent years for cost-effective, large area and flexible electronic device production, encouraging the development of new applications [1-4]. Researchers have investigated different methods to enhance transistor performance; some examples are the improvement of the semiconductor-insulator interface [5,6], the introduction of additional organic layers [7,8], the use of efficient contact materials [9,10] and the fabrication process optimization [11,12]. However, the theoretical interpretation of their electronic and optical properties is not always straightforward. The large variety of organic semiconductors and their particular sensitivity to various elements and composites make OTFTs a good candidate for low-cost and selective chemical and physical sensors [13,14]. Conversely, for applications when enduring stability is required, it is fundamental to reduce the suffering due to the exposure to external factors, such as humidity, electric field and light, which could induce an unwanted chemical degradation and a reduction of the device performance [15].

Since OTFTs can be integrated in optoelectronic applications, as part of the driving circuitry of displays, or used as photo-detectors or light-activated memory devices, it is important to understand the effect of illumination on their electrical performance [16-18]. Recently, organic phototransistors (OPTs), where the control of channel conductance can be enabled by both the magnitude of gate voltage and the absorption of light, have attracted considerable attention thanks to the good response time and the higher responsivity with respect to organic photodiodes [19]. The combination of the organic semiconductor and the gate dielectric plays a key role to determine the performance of OPTs. In particular, it is essential to employ organic semiconductors with both high mobility and excellent

light sensitivity and to exploit polymer dielectrics that yield low gate leakage currents and the proper surface for the semiconductor growing.

Pentacene, which is one of the most studied p-type organic semiconductor, has found application in OPTs thanks to its high electrical performance and absorption properties with a great generation efficiency in a wide wavelength region [20-22]. A pentacene-based transistor subjected to light excitation exhibits a behavior depending on the photon energy. Under white or low energy ultraviolet (UV) light, an enhancement of the saturation current, a positive shift of the threshold voltage and a reduction of the total trap density with increasing illumination intensity were reported [23]. In particular, in TFTs with pentacene deposited on polymer dielectrics, permanent effects were observed after a low energy UV treatment, which was therefore proposed as a simple way of enhancing the general performance of transistors and controlling their threshold voltage [24]. The photosensing properties of a pentacene OPT are mainly affected by the dielectric surface, which impacts the interface trap density [25], and it was seen that a thinner dielectric layer with a smooth surface is essential for an efficient transport in the channel and enhances photosensitivity [26]. Higher performance under illumination was also observed by reducing the thickness of the pentacene active layer [27] or by introducing a fullerene buffer layer under the electrodes [28].

The present study is devoted to the investigation of photocurrent in OTFTs fabricated with pentacene deposited on a photocurable polymer. The comparison between the electrical characterizations in dark and the results obtained under light conditions has yielded the development of equations useful to describe the photocurrent evolution and to distinguish the effects of photogenerated electrons and holes. Upon light absorption, a high concentration of free charges is induced by exciton generation. In particular, photoinduced holes flow to electrodes, giving a direct contribution to the photocurrent. Conversely, electrons escaped from exciton recombination near the insulator interface, due to the lower mobility, become trapped inducing a positive shift in the threshold voltage. Thus, thanks to the large concentration of both charge carriers generated by light, the measurements performed under photoirradiation allow the identification of trap states affecting charge transport. At the same time, it is possible to evaluate the stability of the electrical performance of the organic transistors under steady-state illumination and to assess the applicability of such devices as photodetectors. However, the measurements under illumination depend on the testing conditions. In our case, a measurement-induced effect has been found as a result of the prolonged application of a gate bias under photoirradiation.

2. MATERIALS AND METHODS

Our organic thin film transistors were fabricated in the top-contact bottom-gate configuration, starting from a glass substrate. A transparent gate electrode of ITO (Indium-Tin-Oxide) was deposited with a thickness of 125 nm. A photocurable polymer by Polyera Corporation (ActivInk D0150) was used as gate insulator. The polymeric solution was spin-coated to afford a film thickness of about 600 nm. The film was cured under ultraviolet irradiation at 300 nm wavelength to activate a cycloaddition process (Fig. 1). The degree of bulk crosslinking was monitored by the optical absorption spectroscopy of the corresponding film on a quartz substrate, in particular through the evaluation of the progressive absorbance decrease of a peak at 270 nm, assigned to the cinnamoyl fragment [29]. The film was irradiated for 30 min and then baked at 120°C for 2 min. Subsequently, thermal evaporation of a 50 nm thick pentacene active layer was conducted with a base pressure of $2 \cdot 10^{-7}$ mbar. The deposition rate of the organic molecule was maintained at 0.5 Å/s while the substrate was kept at room temperature. After semiconductor film deposition, the transistors were completed by evaporating a 50 nm thick layer of gold through a shadow mask to realize source and drain electrodes.

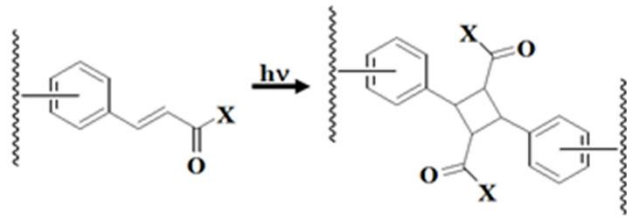


Figure 1. Schematic of the cycloaddition reaction occurring in ActivInk D0150 film via photocrosslinking.

AFM images and height profiles of the polymer surface (Fig. 2) were recorded, showing that the resulting films are very smooth with a root-mean-square roughness less than 0.3 nm. Several samples of ITO/D0150/Au capacitors were fabricated in order to evaluate the leakage current density as a function of the electric field. The J - E curves (Fig. 3) reveal very low leakage current densities across the insulator, with values smaller than 10^{-8} A/cm² at 3 MV/cm in most cases. Thanks to the capacitors, the dielectric constant of the polymer was determined to be 3.3.

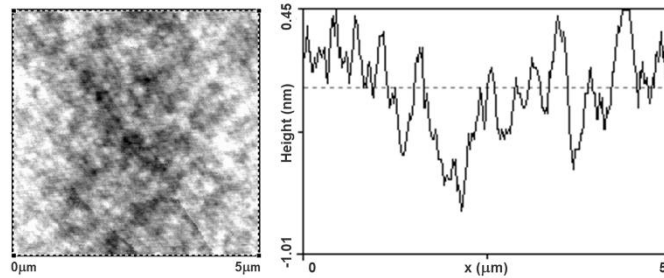


Figure 2. AFM image and height profile of a D0150 film deposited on glass/ITO.

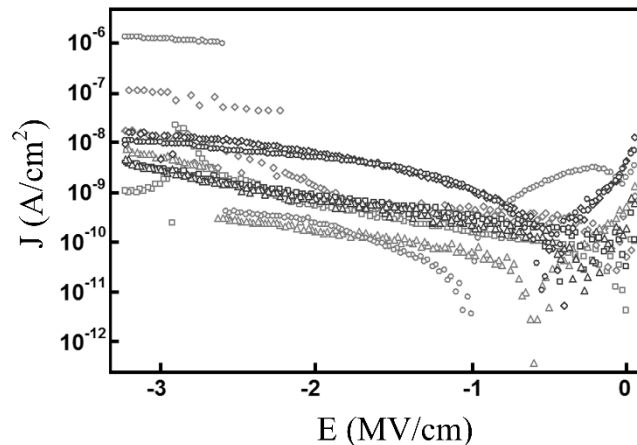


Figure 3. J - E curves of similar ITO/D0150/Au devices (8 samples). Leakage currents are smaller than 10^{-8} A/cm², except for two samples.

Transistors were characterized at room temperature, both in dark and under light conditions, and fundamental parameters were estimated. Many devices were considered; since they showed similar features, typical results are reported. In order to investigate the effects of the incident light on the OTFT performance, the devices were illuminated from the top side, by using LEDs located at a distance of 5 mm from the substrate. Wavelengths covering the visible and ultraviolet range between 285 nm and

630 nm and various irradiances were used. Light with energy lower than HOMO-LUMO gap of pentacene (1.97 eV) did not affect the devices significantly and their results are not reported [19,21,30].

It was seen that both the measuring method and the bias application time affect the performance parameters. In particular, after each measurement, the device seemed to switch on with less negative threshold voltage. This behavior can be attributed to the exposure to ambient air; indeed, by keeping the devices in vacuum for at least 12 hours it was possible to partially regain the original features, reasonably due to the release of oxygen, which had been absorbed from the atmosphere enhancing film conductivity by acting as dopant for pentacene [31,32]. After about four months, the repeated bias stress, as well as the inherent degradation process essentially due to moisture absorption, tended to modify permanently the transistor behavior (Fig. 4) [33]. Because of bias stress, also an increased leakage current through the insulator (by a factor of 3) was detected.

The exposure to irradiation, especially to ultraviolet light, altered the electrical characteristics even more incisively. The results were a transconductance decrease and a threshold voltage shift toward larger positive values, so that the saturation regime was no longer observed within the bias range considered during the first electrical characterization, as it is evident in the transfer characteristics of Fig. 4(a). On the contrary, the exposure to a UV light had a positive effect on the insulator; indeed, an irradiation centered at a wavelength (285 nm) close to the one used for the dielectric curing (300 nm) was revealed to restore the pristine values of the gate leakage.

On the time scale of these experiments, it seems that in dark molecular oxygen does not react irreversibly with pentacene and that also a visible light excitation is not sufficient to promote a reaction, so that oxygen, diffused into pentacene at atmospheric pressure, can evacuate rapidly under vacuum, according to experimental results found in literature [33]. In contrast, the exposure of pentacene to air in presence of UV light most probably yields an oxidation by singlet oxygen and/or ozone produced by UV light [24,35].

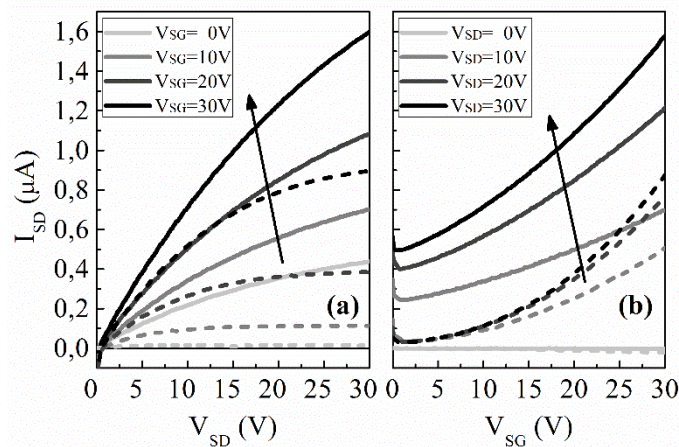


Figure 4. Output (a) and transfer characteristics (b) of pentacene-based OTFTs. Pristine samples (dashed lines) and after repeated bias and optical stress over about four months (solid lines).

3. EXPERIMENTAL RESULTS

The electrical characteristics collected in the dark and under light conditions are compared. An example is reported in Fig. 5, where the transfer curves of an OTFT working in linear region are shown.

The dark current I_d of a thin film transistor can be described by the equation:

$$I_d = \frac{W}{L} \mu_{FE} C_i (V_{GS} - V_T) V_{DS}, \quad (1)$$

where W and L are the width and the length of the channel, respectively, C_i is the insulator capacitance, V_{GS} and V_{DS} are the voltages at gate and drain electrodes related to the source potential, V_T is the threshold voltage, μ_{FE} is the field effect mobility in linear region, i.e. the charge carrier mobility estimated from the slope of the curve $I_d - V_{GS}$. However, in our case the actual transfer curves of the fabricated devices deviates from straight lines and a dependence of the field effect mobility on the gate bias has to be supposed. In particular, the mobility through the conducting channel increases with the gate voltage, reaching the value of about $3 \cdot 10^{-2} \text{ cm}^2/\text{V}$ at $V_{GS} = -30 \text{ V}$.

Thanks to the photo-generation of mobile charge carriers, the current detected under irradiation is higher than the dark current. In a field-effect transistor, illumination could be an element able to control the channel conductance, similarly to the voltage applied to the gate electrode, that is, an optical control signal is added to the electrical signal [22,36]. A gate-to-source voltage that biases the device in its on-state causes the conduction to be dominated by field-induced charges even under illumination, while, below the threshold voltage, the main part of the measured current is given by light-induced charges and the photoresponse is greater than in accumulation regime. In other words, the thin film transistor could be switched on through two control elements, a gate voltage or a light radiation, and when one of these sources is off the effect of the other one is maximized.

The transfer curves measured under illumination, as shown in Fig. 5, display a shift toward more positive gate voltages with respect to the transfer characteristics in the dark. Such a behavior is similar to that induced by dark bias stress [33,37] and, in our case, has been justified by the presence of deep states in the channel region at the insulator-semiconductor interface. Indeed, when charge carriers are trapped at the interface, they can partially screen the gate field, leading to a translation of threshold voltage. This shift allows the estimation of surface deep trap density, but it can mask a possible change in conductivity, which is rather affected by shallow traps.

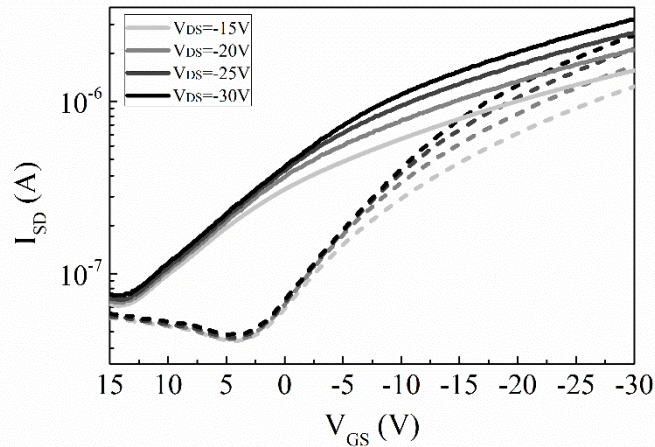


Figure 5. Transfer curves of an OTFT in dark (dashed lines) and under illumination (solid lines) at V_{DS} from -15 V to -30 V.

Different behaviors were revealed depending on the radiation energy and optical power. In particular, if the devices are irradiated with a visible light source (between 470 and 630 nm), their characteristic curves exhibit a positive shift along the voltage axis, with the greatest effect at a photon energy near the absorption edge of the organic semiconductor. Moreover, the photocurrent, defined as the current increase under light conditions, raises with irradiance level. On the other hand, when transistors are

illuminated with an ultraviolet light source, the threshold voltage shift is even larger but the photocurrent drops when optical power is high. The irradiance dependence of the photocurrent, normalized to the dark current, in the case of UV light is illustrated in Fig. 6, at different gate-to-source voltages.

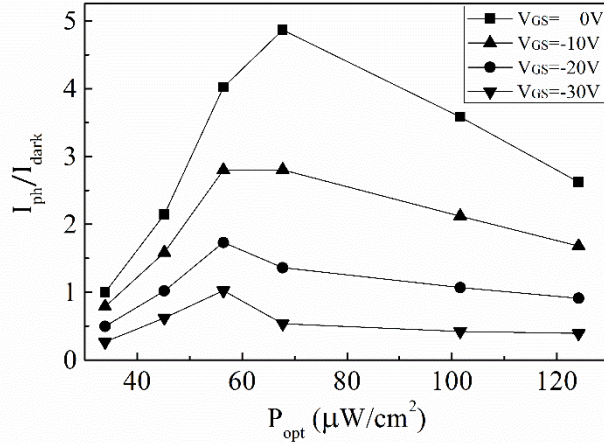


Figure 6. Dependence of the photosensitivity ($V_{DS} = -20\text{ V}$) on the irradiance of an ultraviolet irradiation at various V_{GS} .

Besides the relationship between the photocurrent and the irradiance, the time evolution of the current, both during and after irradiation, was inspected. The drain current was collected after holding the bias for 10 s, at a fixed drain voltage and four different gate voltages. The results are reported in Fig. 7. The current gradually increases under light irradiation, while a persistent photocurrent is observed when light is turned off and the current relaxes back toward its original value with long time constants. However, the behavior depends on the gate voltage applied during measurements; it was found that for higher negative gate biases the light source removal yields an initial increase in current before the decay of the persistent photocurrent. Such a phenomenon appears to be induced by polarization; in particular, a high negative gate bias produces a process that compensates the light-induced effects, yielding a negative photocurrent when light is turned off. For the same reason, also collection of current-voltage characteristics under light conditions is almost certainly affected and made unreliable by bias stress. This phenomenon has been demonstrated by changing the ramp speed of the gate voltage for the transfer curve: indeed, lowering the sweep rate from 3 V/s to 0.2 V/s, the current curves under illumination tend to stretch out, so that the resulting photocurrent reduces to zero (Fig. 8).

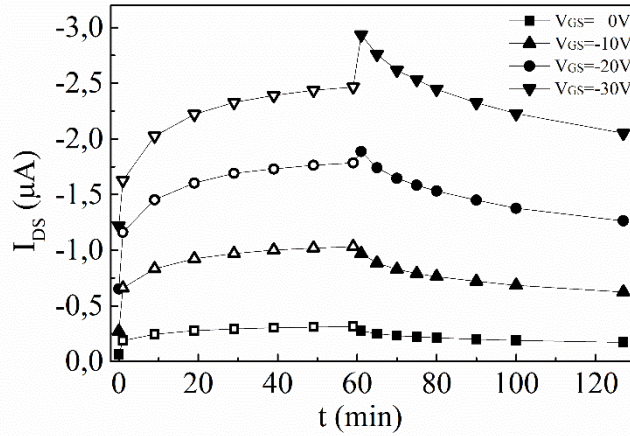


Figure 7. Evolution of drain current under irradiation (open symbols) and recovery in the dark ($V_{DS}=-20$ V) (full symbols). Light was removed at $t=60$ min.

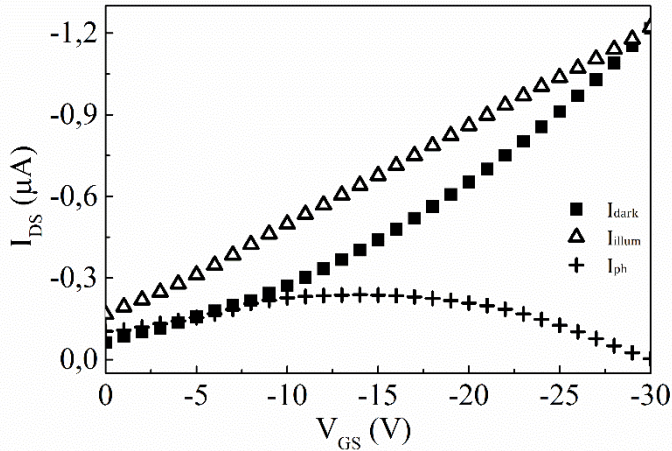


Figure 8. Transfer curves of the OTFT ($V_{DS}= -20$ V) in dark and under illumination with a sweep rate of 0.2 V/s. A measurement self-induced effect is illustrated. By reducing the sweep rate, photocurrent could drop to zero.

4. DISCUSSION

In an organic semiconductor, a large number of excitons are generated when photons of energy equal or higher than the band-gap are absorbed. Subsequently, in the case of pentacene, while holes can flow to the drain electrode, electrons could be easily trapped in localized states due to the lower mobility. Both holes and electrons are responsible, in this way, for an increase in the drain current of an OTFT.

In this regard, two mechanisms have been reported to occur in the active layer to explain the photoinduced response in a field effect transistor [38]. A photovoltaic effect can be observed when the transistor operates in the on-state; it is associated to a photovoltage induced by the accumulation of a large number of carriers under the electrodes, leading to the lowering of the potential barrier between the electrodes and the semiconductor channel [39], and at the interface with dielectric film [17]. This effect can give rise to a significant increase in current, through a shift of the switch-on voltage. A logarithmic relationship describes its dependence on the illumination irradiance:

$$I_{ph,on} = \frac{AkT}{q} \ln \left(1 + \eta_\lambda \frac{qP_{opt}}{hvI_d} \right), \quad (2)$$

where η_λ is the external quantum efficiency, P_{opt} is the incident optical power, h is the Planck constant, ν is the irradiation frequency, I_d is the dark current, kT/q is the thermal voltage and A is a fit parameter.

On the other hand, a photoconductive effect can be seen when the device operates in the off-state. It arises from the photogeneration of mobile carriers, whose number increases with the photon flux, so that the photocurrent exhibits a direct dependence on the illumination power through the following relation:

$$I_{ph,off} = \eta_\lambda G \frac{qP_{opt}}{hv}, \quad (3)$$

where $G = \tau/t_t$ is the photoconductive gain, i.e. the ratio of the carrier lifetime to the transit time.

Starting from these observations, in the present work the total photocurrent I_{ph} measured in the pentacene-based OPTs is assumed to result from the sum of a contribution caused by the threshold shift, $I_{ph,\Delta V_T}$, and a current due to the primary photoconductivity, $I_{ph,pr}$, so that the total current measured under illumination, I_{illum} , is:

$$I_{illum} = I_d + I_{ph} = I_d + I_{ph,\Delta V_T} + I_{ph,pr}, \quad (4)$$

where I_d is the dark current. $I_{ph,\Delta V_T}$ and $I_{ph,pr}$ are introduced, as will be shown hereafter, to take into account the effects of the photogenerated electrons and the photogenerated holes, respectively, on the drain current. Considering the absorption coefficient of pentacene and the thickness of semiconductor film, it is assumed that, under illumination, excitons are generated uniformly in the bulk of the organic layer and then split into free charge carriers. The photogenerated holes give a direct contribution to the photocurrent through the drain, while the photogenerated electrons are trapped in localized states, most likely present at the interface between the pentacene and the insulating layer. When electrons are trapped, they screen the voltage applied at the gate electrode, leading to a translation of the voltage needed to turn on the device. The shift occurs toward more positive voltages, promoting the device switching and increasing the overall channel current.

The effect of irradiation was investigated when the transistors were biased in the linear region, in order to have a channel with a nearly uniform charge carrier concentration from source to drain. For the fabricated OTFTs, Eq. (1) cannot be used with a constant field effect mobility because of the dispersive conduction mechanism, typical of polycrystalline organic semiconductors. Indeed, transfer curves do not exhibit a linear trend and more than one value for the mobility can be defined depending on the selected range of the gate voltage. While in an amorphous organic semiconductor the gate bias dependence of field effect mobility can be related to the hopping charge transport, in polycrystalline films of small-molecule semiconductors, where most of the defects are concentrated at the grain-boundaries, it is more reasonable to attribute this behavior to a multiple trapping and release mechanism. According to this theory, charge transport occurs in a delocalized band but is limited by the intra-gap trap distributions. While majority charges are accumulated in the organic layer upon applying a negative gate bias, localized states are increasingly filled by the shift of Fermi level, thus resulting in an effective mobility dependence on bias. In this case, the field-effect mobility can be defined through the following expression [40]:

$$\mu_{FE} = \mu_0 (V_{GS} - V_T)^\gamma, \quad (5)$$

where μ_0 is the low field-effect mobility, when $V_{GS} = V_T$, and the exponent $\gamma = 2(T_0/T - 1)$ is a semi-empirical parameter, dependent on the temperature T and associated to the width of a band tail distribution represented through a characteristic temperature T_0 .

According to this expression, the dark current, I_d , has a superlinear dependence on the transverse field and it was written as:

$$I_d = K (V_{GS} - V_T)^{\gamma+1} V_{DS}, \quad (6)$$

with $K = \mu_0 C_i W/L$. The exponent γ , obtained from the fitting of the current plot in the dark, is 1.2, equivalent to a band tail width of about 40 meV. The parameter μ_0 is about $2 \cdot 10^4 \text{ cm}^2/\text{V}^2 \cdot \text{s}$.

Thus, in the proposed model, the drain current in the linear regime under illumination was represented through two components:

$$I_{illum} = K_L (V_{GS} - V_{TL})^{\gamma+1} V_{DS} + G_L (V_{GS} - V_{TL})^\gamma V_{DS}. \quad (7)$$

The first term, where K_L and V_{TL} are the equivalent prefactor and threshold voltage under light conditions, resembles the form of the dark current and corresponds to the sum of I_d and $I_{ph, \Delta V_T}$ in Eq. (4). The second term, where G_L is a constant correlated to the pentacene layer conductance under illumination, represents the primary photocurrent $I_{ph, pr}$. The mobility dependence on the transverse electric field has been included in both contributions, by using Eq. (5) with the equivalent threshold voltage under illumination.

The direction of the threshold voltage shift reveals that it results from the trapping of photogenerated electrons, whereas the excess mobile holes can supply a direct photocurrent through the drain, proportionally to the incident light intensity. In particular, supposing that electron trapping occurs mainly in the channel region at the insulator-semiconductor interface, threshold voltage translation ΔV_T can be related to trapped electron surface density, n_{it} , through the insulator capacitance:

$$\Delta V_T = V_{TL} - V_T = \frac{q n_{it}}{C_i}, \quad (8)$$

while the constant G_L is related to the photogenerated charge carriers, n_{ph} , in the semiconductor layer and it can be written as:

$$G_L = \frac{q \mu_0 n_{ph}}{L^2} = \frac{q \mu_0 \tau}{L^2} \eta_\lambda \frac{P_{opt}}{h\nu}, \quad (9)$$

where τ is the excess carrier lifetime.

The experimental data collected in the dark, during and after irradiation, were fitted to the proposed equations. The typical behavior of a transfer curve in the linear region is shown in Fig. 9. The value of γ , which describes the superlinear trend of curves in dark due to trap states, is also used for the fitting of curves under light conditions. While common parameters, such as threshold voltage, field-effect mobility and subthreshold slope, measured under light conditions are mutually reliant, the parameters K_L , V_{TL} and G_L , thus defined in this model, are independent and allow to investigate separately the light effect on the pentacene structure, the trapping of excess electrons and the photoconductive efficiency. These parameters were extracted from Eq. (7) and their evolution with illumination time were studied.

The dependences of each component on exposure time, as well as recovery kinetics, were recorded for different photon energies. The typical results are shown in Fig. 10 for a visible light radiation and in Fig. 13 for a UV light.

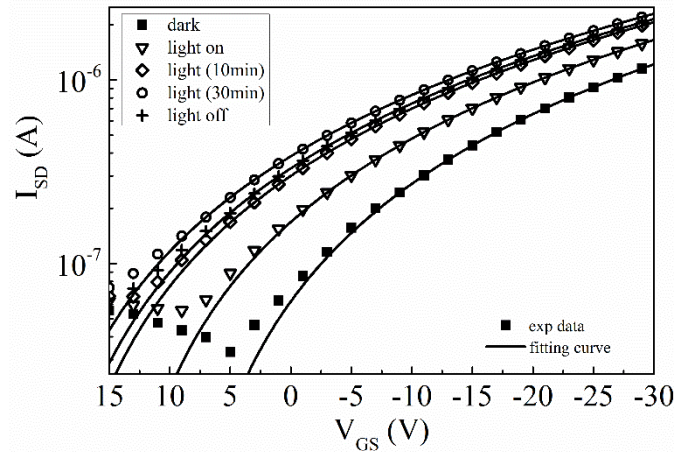


Figure 9. Typical transfer characteristics of the OTFT ($V_{DS} = -20$ V) in dark, at different illumination times and after irradiation. Experimental data were fitted with Eq. (7) of the proposed model.

Regarding the effects of an irradiation in the visible range (Fig. 10), during illumination, a gradual shift of the threshold voltage is observed, suggesting that electrons are trapped at the interfaces. Meanwhile, the low field mobility, μ_0 , extracted from the parameter K_L , remains practically constant, indicating that the structure of the organic semiconductor is not affected by visible illumination. As stated previously, this parameter does not depend on threshold voltage, differently from field-effect mobility, which rather increases under illumination due to the reduction of inter-grain barrier height in the organic semiconductor [21]. The response of photogenerated holes, as seen in the evolution of the photoconductance parameter G_L , is limited by the dispersive transport in the organic material [41].

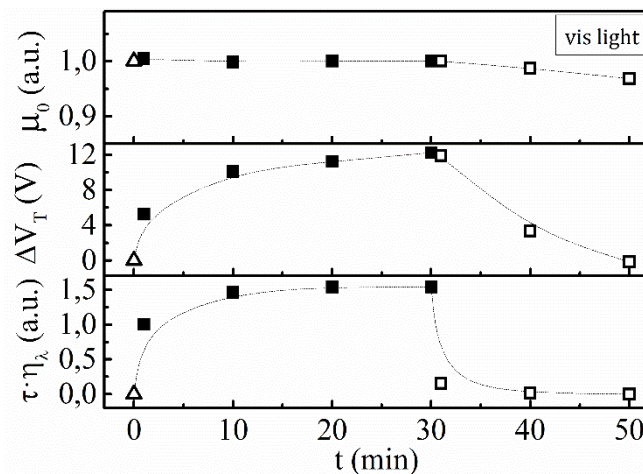


Figure 10. Evolutions of low field-effect mobility (μ_0), threshold voltage shift (ΔV_T) and the product $\tau\eta_x$ extracted from photoconductance factor (G_L) in dark (Δ), during visible light (590 nm) irradiation (\blacksquare) and after irradiation (\square).

As regards the recovery of current after visible irradiation, it is evident that, while the primary photocurrent disappears within a few tens of seconds, the current remains at an elevated level due to the photovoltaic effect. The trapped electrons, responsible for this behavior, recombine with time constants of the order of 10^3 to 10^4 s. A full recovery of the initial properties is not always observed. In some cases, an intrinsic degradation of the conductivity due to the air exposure is observed before the light induced effects could disappear.

It is worthy to point out that the curves of the threshold voltage shift could be well fitted with a power law $\Delta V_T \sim t^\alpha$, where t is the illumination time and α depends on the maximum gate voltage achieved during measurements. The power law could be an approximation in the short time range of the stretched-exponential equation commonly used to describe charge trapping induced by bias and illumination stress [42]. In our case, the exponent α ranges from 0.22 for $V_{GS,max} = -50$ V to 0.31 for $V_{GS,max} = -20$ V, that is, the translation in V_T is slower for high negative V_{GS} (Fig. 11). The reasons could be the repulsion of photogenerated electrons from the interface where they are trapped and the enhanced recombination of holes. This hypothesis can justify the suppression of photocurrent during the recording of transfer characteristics, as seen in Fig. 8, when the device is stressed with a high negative gate voltage for a long time. Indeed, since interface trapping of excess electrons is supposed to be responsible for the forward shift of threshold voltage under illumination, a negative gate bias drives electrons far from interface, leading to a temporary backward shift of the threshold voltage during the I-V measurement itself. Furthermore, as more holes are driven to the insulator-semiconductor interface, the probability of hole trapping in deeper states is enhanced. Thus, at a low sweep rate, the current curves under illumination are stretched, due to the competition of the photovoltaic and photoconductive effects.

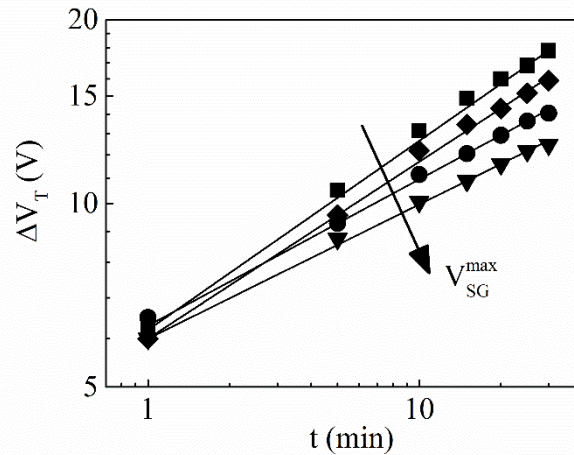


Figure 11. Light-induced threshold voltage shift after different illumination times, as a function of the maximum gate voltage achieved during measurements (V_{SG} from 20 to 50 V).

In order to verify this phenomenon, a prolonged constant bias was applied to the gate of the OTFT under illumination between consecutive measurements. The transfer characteristics were observed in dark after a 5 min illumination, during which the source and drain electrodes were grounded and gate was stressed with a positive or negative bias (Fig. 12). When a positive gate bias is applied, an accelerated light-induced threshold shift toward positive values is revealed, since photo-generated holes can flow from organic semiconductor to electrodes. On the contrary, a negative gate bias reduces the threshold voltage translation induced by illumination to such an extent that for higher negative values

the shift changes its direction. In this case, the photo-generated holes are confined in the channel and could easily recombine with the light-induced electrons. In other words, the prolonged gate polarization with a negative bias works against the light induced effects and the threshold voltage moves toward more negative values, as observed under positive drain bias stress in dark [37]. These effects, obtained as a result of the illumination of the devices and the simultaneous application of an electric field perpendicular to the interface, partly justify the current evolution illustrated in Fig. 7. Indeed, it is evident that a high negative gate bias applied for 10 s temporarily suppresses the photovoltaic effect. However, since the effect of negative charge trapping reappears as soon as the light is removed, the responsible mechanism seems rather to be a short-term compensation due to positive charged interface states induced by the negative gate bias.

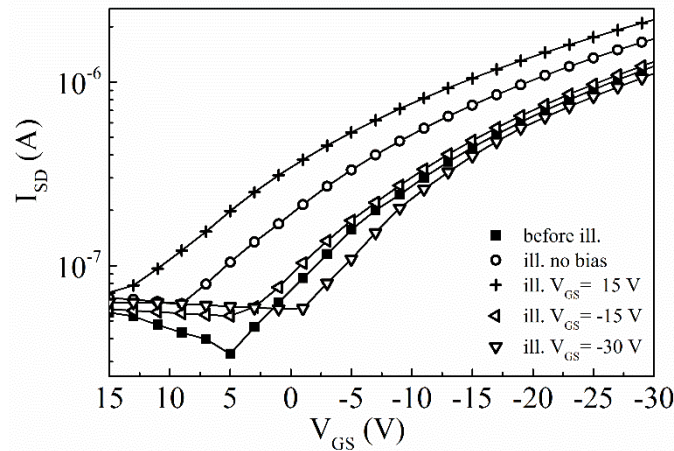


Figure 12. Transfer characteristics ($V_{DS} = -20$ V) before and after illumination. The OTFT was irradiated for 5 minutes without bias or under stress conditions with positive (15 V) or negative (-15, -30 V) gate bias.

Differently from irradiation by visible light, illumination by an ultraviolet source induces a modification in the structure of the organic semiconductor. This is evident from the reduction of the parameter K_L over the whole irradiation period, especially for a wavelength of 285 nm, which is the example shown in Fig. 13. This effect has been attributed to the creation of electrically active defects in pentacene layer [43]. The hypothesis of the increase in photoinduced traps also justifies the evolution of threshold voltage and photoconductivity. Indeed, the threshold voltage shift is not seen to reach an equilibrium value but tends to a continuous growth as long as the light is on, indicating that even more electrons are being trapped. Simultaneously, a decrease in photoconductance is observed; it is faster than the mobility degradation and it is likely due to the enhancement of the hole trapping, as can be seen from the reduction of the product between carrier lifetime and quantum efficiency. The UV light induced defects show a metastable nature and anneal out after the irradiation removal with a time constant of about 10^3 s. However, continual irradiations by UV light modify permanently the material properties.

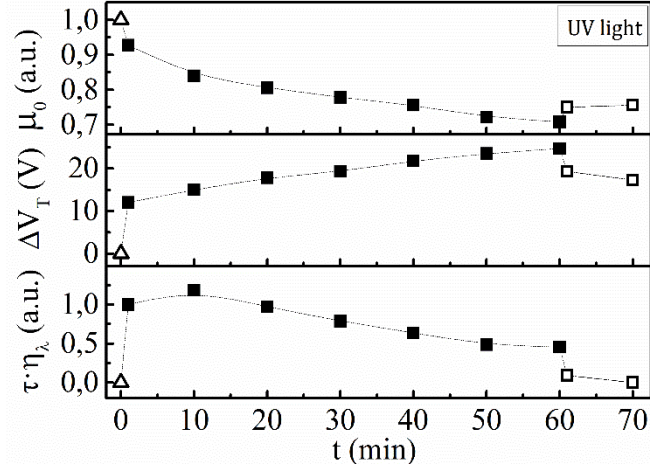


Figure 13. Evolutions of low field-effect mobility (μ_0), threshold voltage shift (ΔV_T) and the product $\tau \cdot \eta_x$ extracted from photoconductance factor (G_L) in dark (Δ), during ultraviolet light (285 nm) irradiation (\blacksquare) and after irradiation (\square).

A comparison of the threshold voltage shift along the entire range of wavelengths is made difficult by the non-linear dependence on the optical power, as well as on illumination time. To overcome this problem the threshold voltage shift can be monitored at a very low power density, so that Eq. (2) is approximated to:

$$\Delta V_T \cong \frac{AkT\eta_x P_{opt}}{hvI_d}, \quad (10)$$

where A is a constant, and a normalization to incident photon flux and dark current is applied in order to evaluate the quantum efficiency (Fig. 14). The highest values in the visible range appear in correspondence to the irradiation energies of 2.1 and 2.3 eV, which are ascribable to the charge-transfer exciton levels of a pentacene thin film. In ultraviolet range, the highest efficiency is measured at 3.4 eV and is connected to the molecular-like levels of constituent pentacenes.

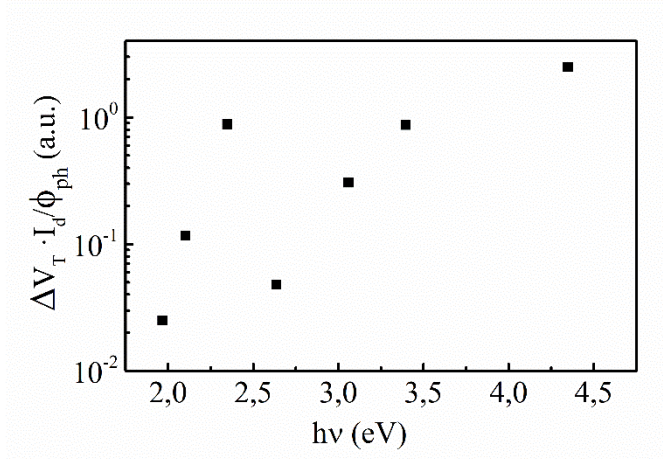


Figure 14. Light-induced threshold voltage shift weighted for incident photon flux density and dark current at different radiation energies. The extracted values are proportional to external quantum efficiency.

While, due to exposure to UV light, the threshold voltage tends to increase to greater and greater values up to the device failure, the maximum shift observed in the threshold voltage upon extended visible illumination is useful for the estimation of the electron surface trap density. Using Eq. (8) with the measured insulator capacitance of 5 nF/cm^2 , the extracted trap state density at the interface with the photocurable polymer is about $9 \cdot 10^{11} \text{ cm}^{-2}$, which is comparable with the values found in literature and slightly smaller than the case of other polymer insulators, such as poly(methyl methacrylate), parylene or poly(4-vinylphenol) [11,17,44,45].

5. CONCLUSION

The current-voltage photoresponse of pentacene-photocurable dielectric-based transistors has been investigated under different conditions. The multiple trapping and release mechanism theory is effective in explaining the gate bias dependence of field effect mobility when the fabricated OPTs are measured in dark and, in this work, it is exploited in the development of the equations modeling device behavior under light conditions. The study of photocurrent in the OTFTs has allowed to distinguish a photovoltaic and a photoconductive effect. The equations proposed in this work were used to investigate these two contributions, that is, respectively, the origin of the threshold voltage shift introduced by irradiation and the photoconductive efficiency in the organic semiconductor.

The presence of long-lived traps at the insulator-semiconductor interface has been discussed. They cause threshold voltage instability and affect the data collection under illumination. However, the ability of storing the information about illumination dose for long time could suggest the use of these transistors as memory devices.

The illumination effectively shifts the threshold voltage of the device, while the field-effect mobility of the charge carriers in the channel remains unchanged. Such a feature indicates the usefulness of the illumination in controlling, similarly to a gate-source voltage, the density of charge carriers in the device; in other words, the transistor could be switched on by applying either a negative gate voltage or a pulse of illumination. Since the photoresponse in an organic transistor shows to be strongly time dependent, in order to compare different devices, especially if employed as phototransistors, it becomes fundamental to have information about the illumination dose and the gate bias during illumination.

Finally, the combination of light-induced effect and gate bias stress has been studied, showing that, while a positive gate voltage accelerates the threshold voltage shift, the photovoltaic effect can be fully suppressed by a negative gate bias. This ability to modulate the light-induced ΔV_T with the gate bias could be exploited to change the sensitivity of organic phototransistors and light-activated memory devices.

ACKNOWLEDGMENTS

Support by SMARTAGS project (PON02_00556_3420580) financed by the Ministero dell'Università e della Ricerca (MIUR) in the ambit of the National Operational Programme for Research and Competitiveness 2007-2013 is gratefully acknowledged.

REFERENCES

[1] G.-S. Ryu, K.-B. Choe, and C.-K. Song, Thin Solid Films 514 (2006) 302-305

- [2] J. Jang, and S. H. Han, *Curr. Appl. Phys.* 6S1 (2006) e17-e21
- [3] M. Fadlallah, G. Billiot, W. Eccleston, and D. Barclay, *Solid-State Electronics* 51 (2007) 1047-1051
- [4] H.F. Castro, E. Sowade, J.G. Rocha, P. Alpium, A.V. Machado, R.R. Baumann, and S. Lanceros-Méndez, *Org. Electron.* 22 (2015) 12-19
- [5] Y. Ha, S. Jeong, J. Wu, M.-G. Kim, V. P. Dravid, A. Facchetti, and T. J. Marks, *J. Am. Chem. Soc.* 132 (2010) 17426-17434
- [6] Z. He, J. Chen, J. K. Keum, G. Szulczewski, and D. Li, *Org. Electron.* 15 (2014) 150-155
- [7] R. Ye, M. Baba, K. Suzuki, and K. Mori, *Thin Solid Films* 517 (2009) 3001-3004
- [8] C.-T. Lee, and Y.-M. Lin, *Org. Electron.* 14 (2013) 1952-1957
- [9] K. Fukuda, et al., *Org. Electron.* 13 (2012) 1660-1664
- [10] H. Gui, B. Wei, and J. Wang, *Org. Electron.* 15 (2014) 3349-3353
- [11] J.-H. Bae, and Y. Choi, *Solid State Electron.* 72 (2012) 44-47
- [12] H. Gold, et al., *Org. Electron.* 22 (2015) 140-146
- [13] M. E. Roberts, S. C.B. Mannsfeld, R. M. Stoltenberg, and Z. Bao, *Org. Electron.* 10 (2009) 377-383
- [14] X. Ren, P. K.L. Chan, J. Lu, B. Huang, and D. C.W. Leung, *Adv. Mater.* 25 (2013) 1291-1295
- [15] S. Bisoyi, U. Zschieschang, M. J. Kang, K. Takimiya, H. Klauk, and S. P. Tiwari, *Org. Electron.* 15 (2014) 3173-3182
- [16] M. Debucquoy, S. Verlaak, S. Steudel, K. Myny, J. Genoe, and P. Heremans, *Appl. Phys. Lett.* 91 (2007) 103508
- [17] C. S. Suchand Sangeeth, P. Stadler, S. Schaur, N. S. Saricifitci, and R. Menon, *J. Appl. Phys.* 108 (2010) 113703
- [18] C. H. Kim, M. H. Choi, S. H. Lee, J. Jang, and S. Kirchmeyer, *Appl. Phys. Lett.* 96 (2010) 123301
- [19] K.J. Baeg, M. Binda, D. Natali, M. Caironi, and Y.-Y. Noh, *Adv. Mater.* 25 (2013) 4267-4295
- [20] Y.-Y. Noh, D.-Y. Kim, *Solid State Electron.* 51 (2007) 1052-1055
- [21] A. El Amrani, B. Lucas, F. Hijazi, and A. Moliton, *Mater. Sci. Eng. B* 147 (2008) 303-306
- [22] F. Yakuphanoglu, and W. A. Farooq, *Synth. Metals* 161 (2011) 379-383
- [23] B. Gunduz, O. A. Al-Hartomy, S. A F. Al Said, A. A. Al-Ghamdi, and F. Yakuphanoglu, *Synth. Metals* 179 (2013) 94-115
- [24] J.M. Choi, D. K. Hwang, J.M. Hwang, J.H. Kim, and S. Im, *Appl. Phys. Lett.* 90 (2007) 113515
- [25] J.M. Choi, S. Im, *Synthetic Metals* 159 (2009) 1689-1693
- [26] J.-H. Kwon, M.-H. Chung, T.-Y. Oh, B.-K. Ju, and F. Yakuphanoglu, *Microelectron. Eng.* 87 (2010) 2306-2311
- [27] A. El Amrani, B. Lucas, and B. Ratier, *Synth. Metals* 161 (2012) 2566-2569
- [28] B. Yao, W. Lv, D. Chen, G. Fan, M. Zhou, and Y. Peng, *Appl. Phys. Lett.* 101 (2012) 163301
- [29] C. Kim, J. R. Quinn, A. Facchetti, T. J. Marks, *Adv. Mater.* 22 (2010) 342-346
- [30] J. Lee, S.S. Kim, K. Kim, J.H. Kim, and S. Im, *Appl. Phys. Lett.* 84 (2004) 1701
- [31] O. D. Jurchescu, J. Baas, and T. T. M. Palstra, *Appl. Phys. Lett.* 87 (2005) 052102
- [32] J. Park, L.-M. Do, J.-H. Bae, Y.-S. Jeong, C. Pearson, M.C. Petty, *Org. Electron.* 14 (2013) 2101-2107
- [33] S. Cipolloni, L. Mariucci, A. Valletta, D. Simeone, F. De Angelis, G. Fortunato, *Thin Solid Films* 515 (2007) 7546-7550
- [34] A. Vollmer, O.D. Jurchescu, I. Arfaoui, I. Salzmann, T.T.M. Palstra, P. Rudolf, J. Niemax, J. Pflaum, J. P. Rabe, and N. Koch, *Eur. Phys. J. E* 17 (2005) 339-343
- [35] H. Yang, L. Yang, M.-M. Ling, S. Lastella, D.D. Gandhi, G. Ramanath, Z. Bao, and C.Y. Ryu, *J. Phys. Chem. C* 112 (2008) 16161-16165

- [36] N. Marjanović, Th.B. Singh, G. Dennler, S. Günes, H. Neugebauer, N.S. Sariciftci, R. Schwödiauer, and S. Bauer, *Org. Electron.* 7 (2006) 188-194
- [37] C.-L. Fan, T.-H. Yang, and C.-Y. Chiang, *IEEE Electr. Device L.* 31 (2010) 887-889
- [38] T. P. I. Saragi, J. Londenberg, and J. Salbeck, *J. Appl. Phys.* 102 (2007) 046104
- [39] C.-S. Choi, H.-S. Kang, W.-Y. Choi, H.-J. Kim, W.-J. Choi, D.-H. Kim, K.-C. Jang, and K.-S. Seo, *IEEE Photonics Technol. Lett.* 15 (2003) 846-848
- [40] G. Horowitz, M. E. Hajlaoui, and R. Hajlaoui, *J. Appl. Phys.* 87 (2000) 4456
- [41] R. Liguori, and A. Rubino, *Org. Electron.* 15 (2014) 1928-1935
- [42] F. R. Libsch, and J. Kanicki, *Appl. Phys. Lett.* 62 (1993) 1286
- [43] R. Liguori, S. Aprano, and A. Rubino, *AIP Conf. Proc.* 1583 (2014) 212-216
- [44] C.-L. Fan, T.-H. Yang, P.-C. Chiu, C.-H. Huang, and C.-I Lin, *Solid State Electron.* 53 (2009) 246-250
- [45] K. K. Ryu, I. Nausieda, D. D. He, A. I. Akinwande, V. Bulović, and C. G. Sodini, *IEEE T. Electron. Dev.* 57 (2010) 1003-1010

Figure1
[Click here to download high resolution image](#)

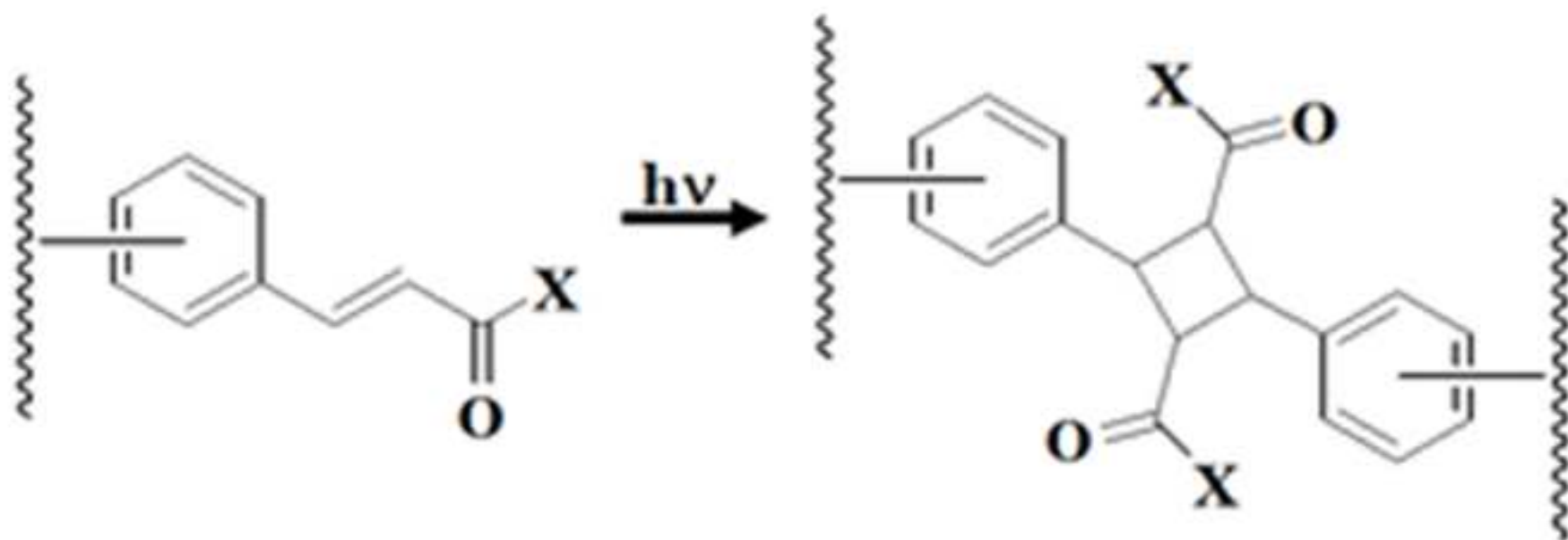


Figure2

[Click here to download high resolution image](#)

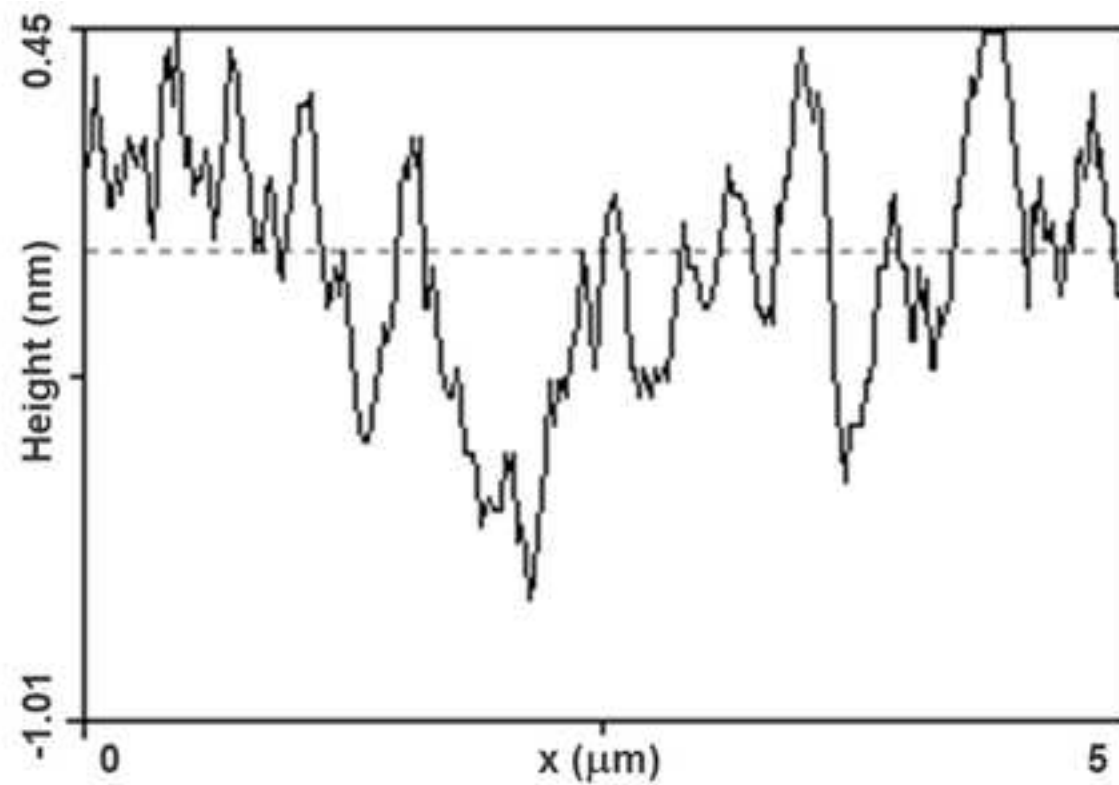
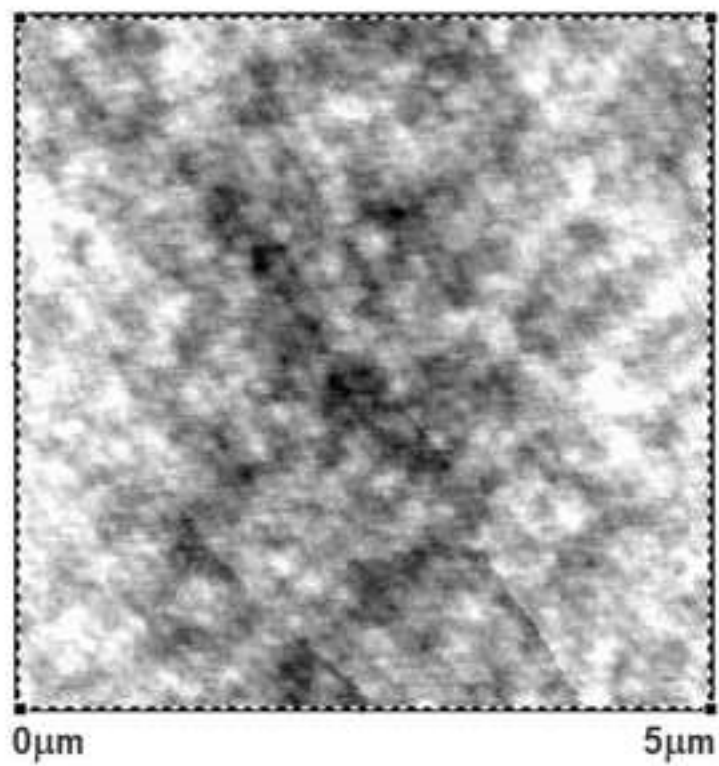


Figure3
[Click here to download high resolution image](#)

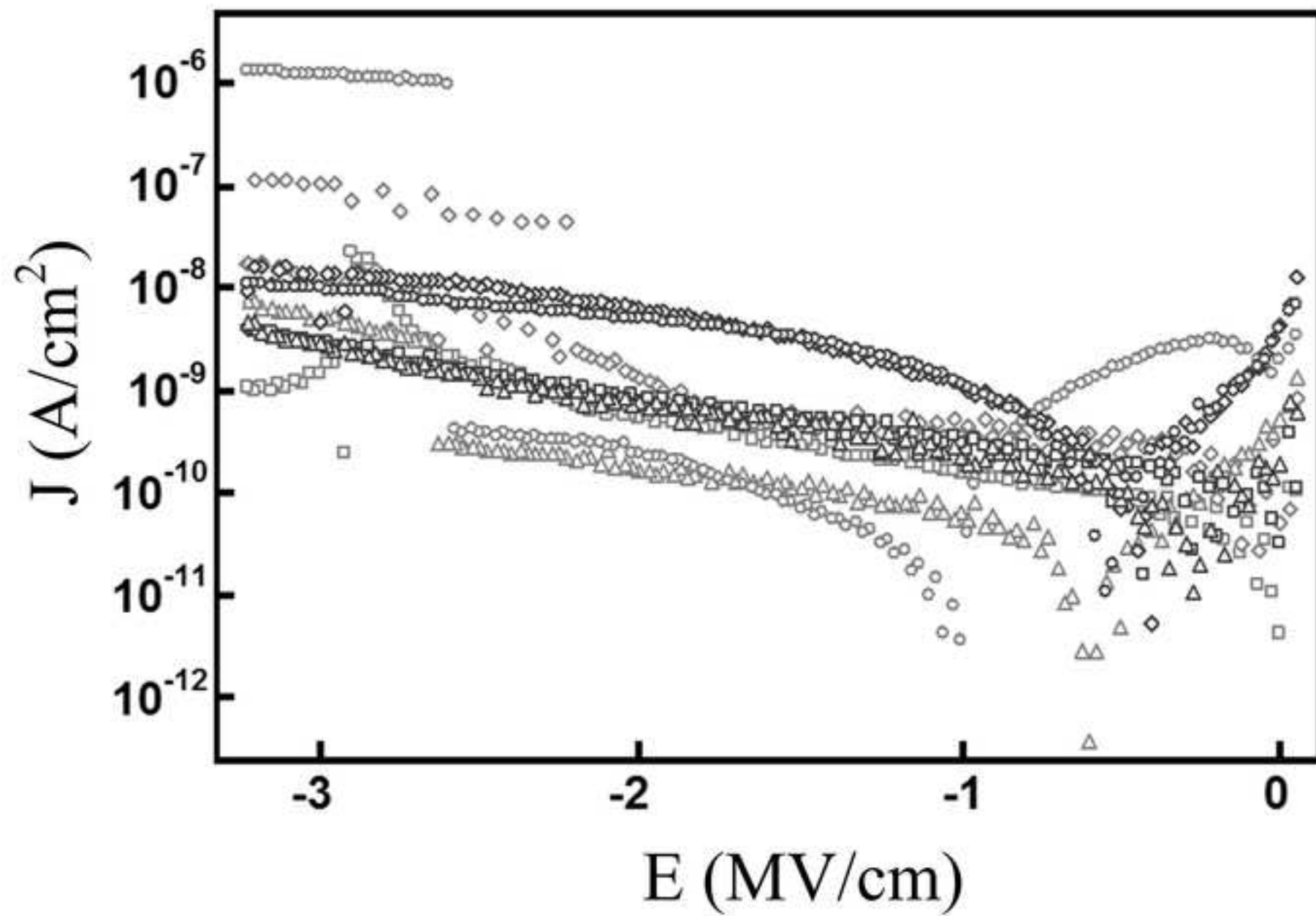


Figure4

[Click here to download high resolution image](#)

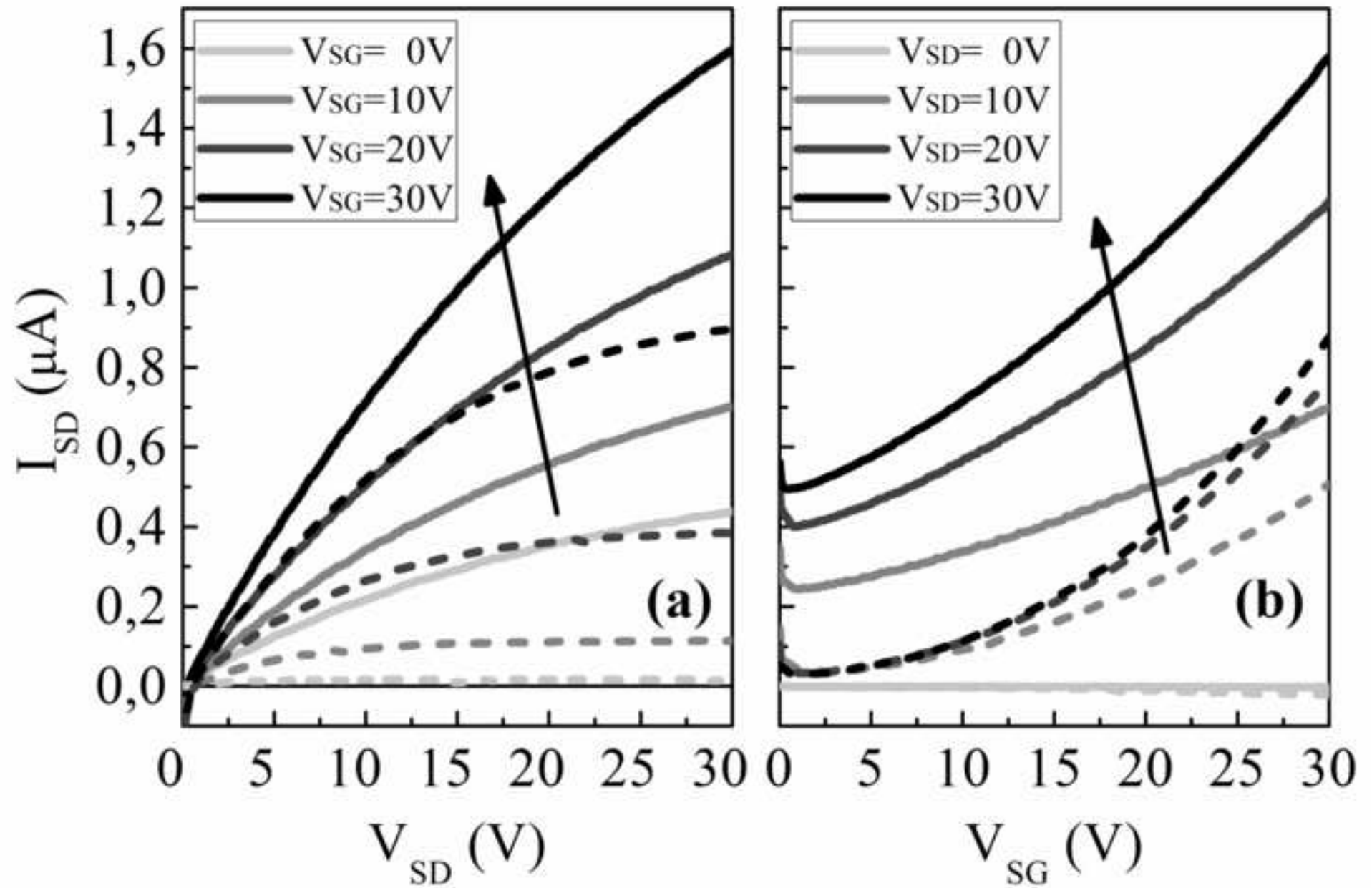


Figure5

[Click here to download high resolution image](#)

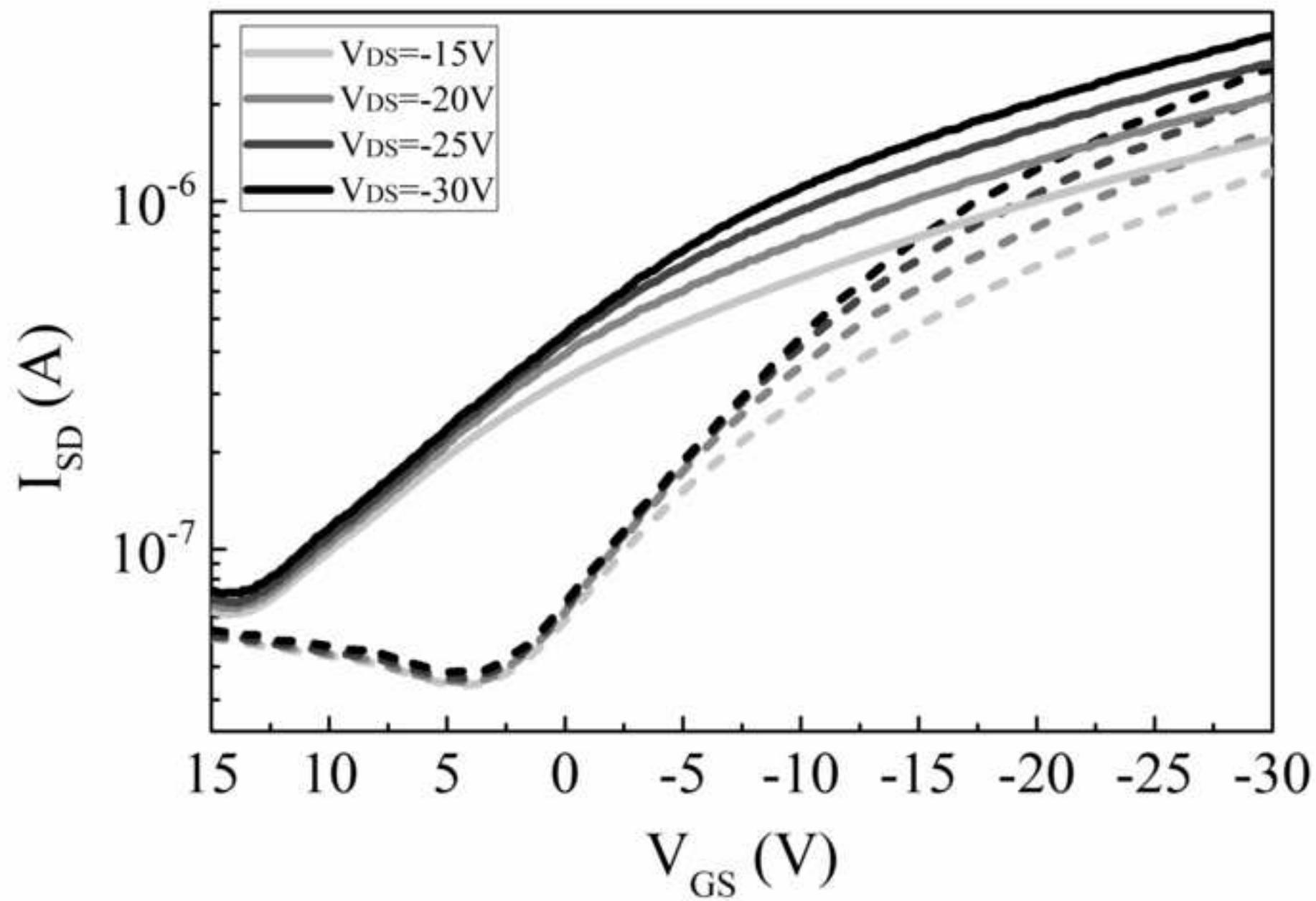


Figure6

[Click here to download high resolution image](#)

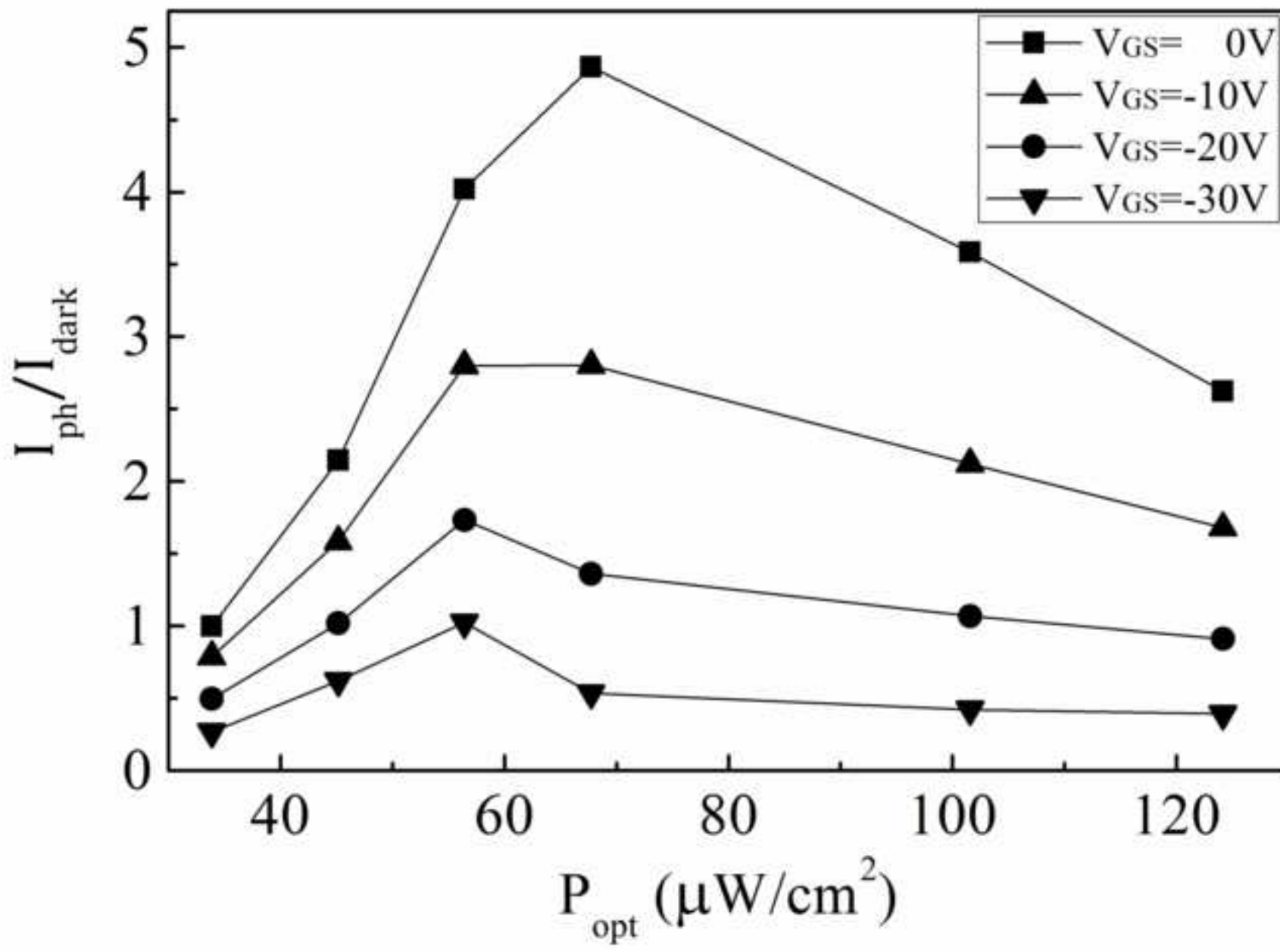


Figure7

[Click here to download high resolution image](#)

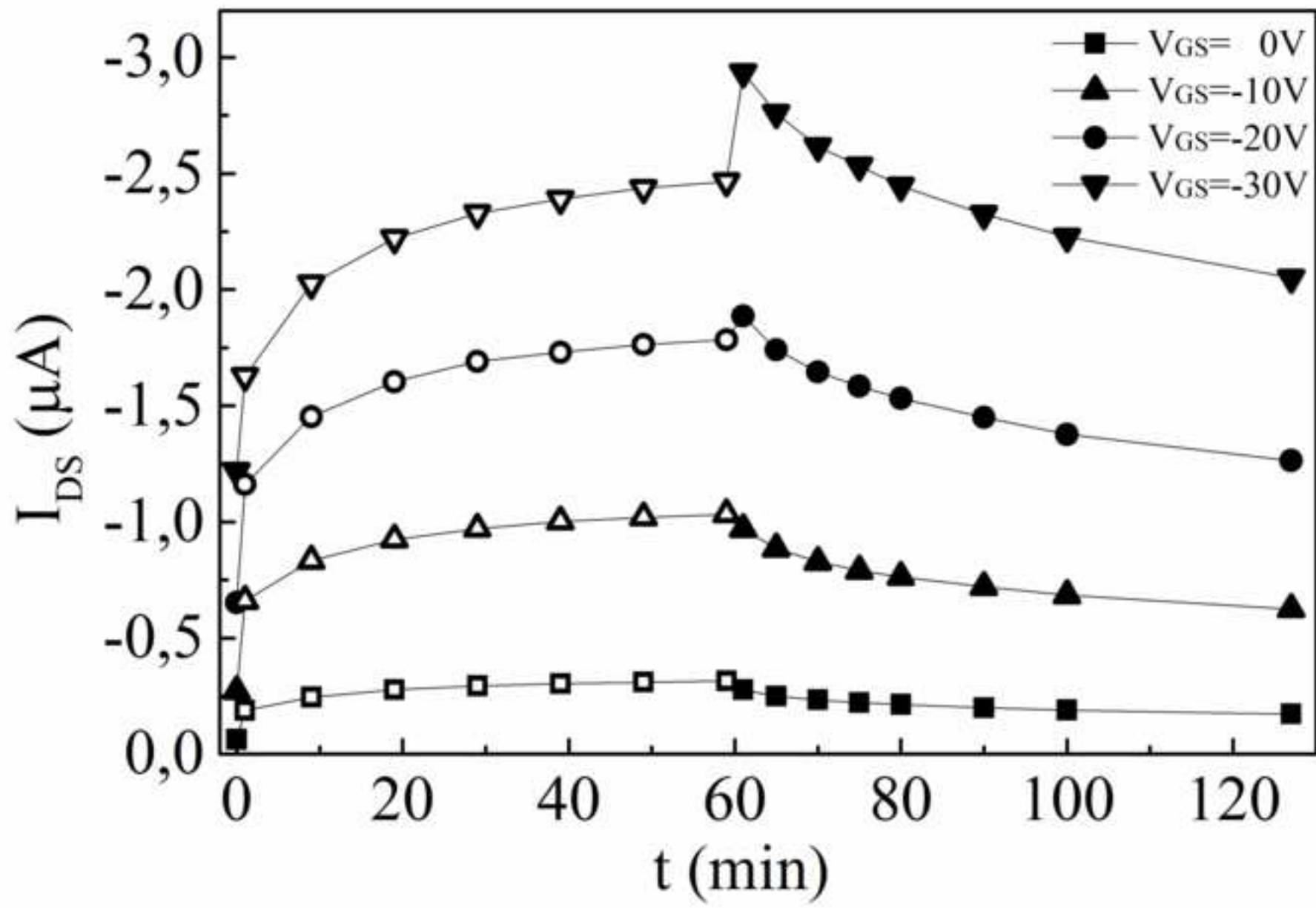


Figure8
[Click here to download high resolution image](#)

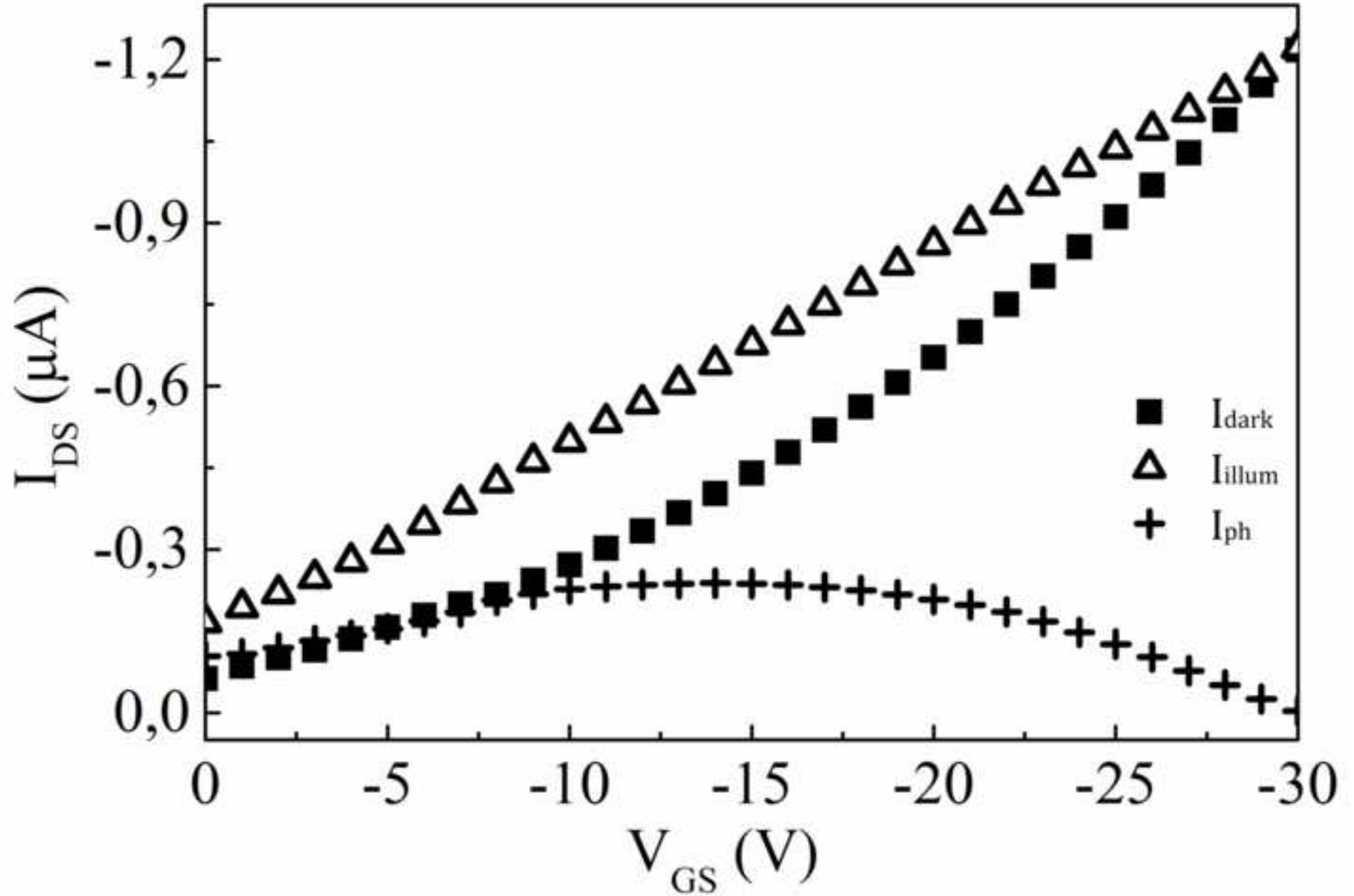


Figure9

[Click here to download high resolution image](#)

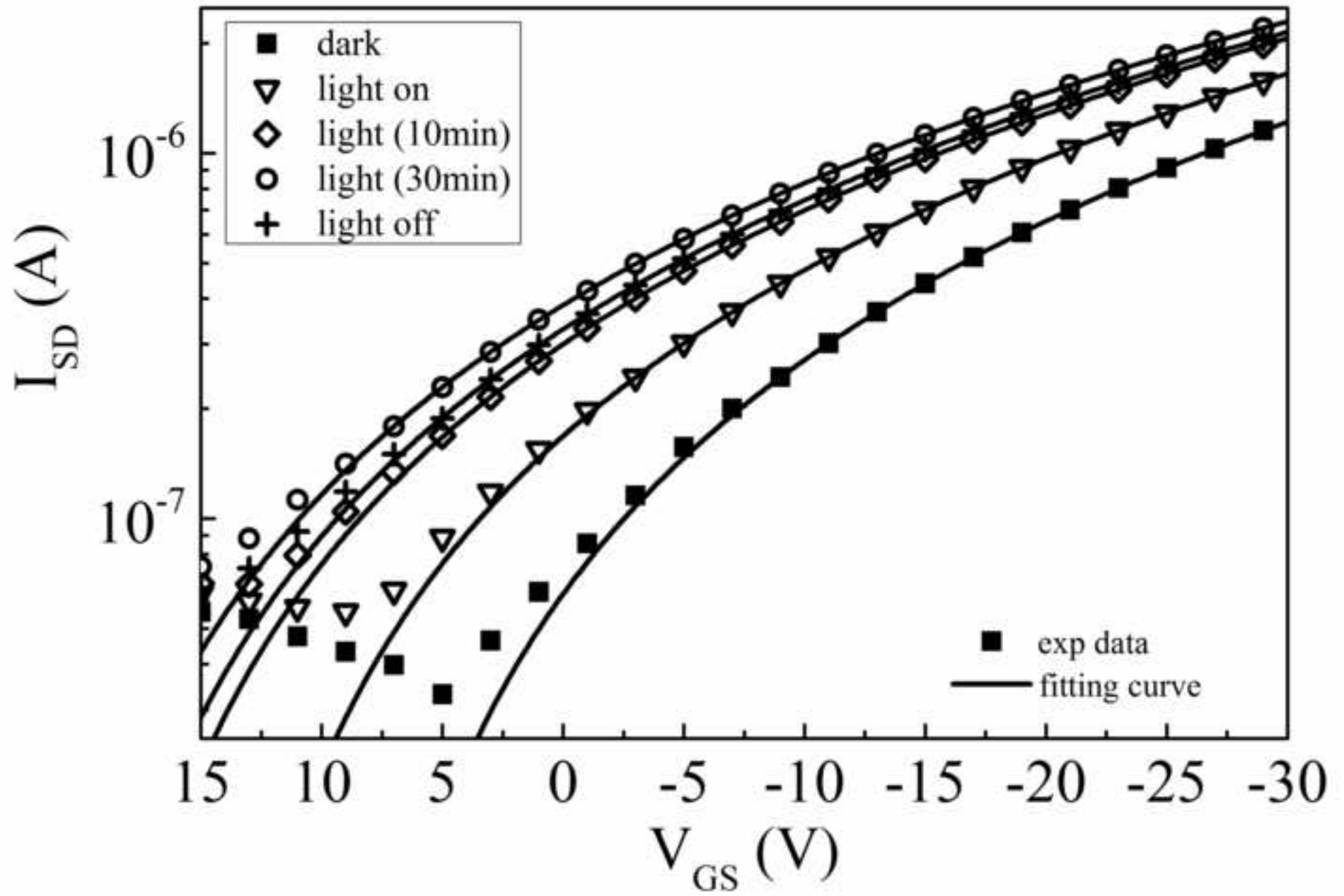


Figure10
[Click here to download high resolution image](#)

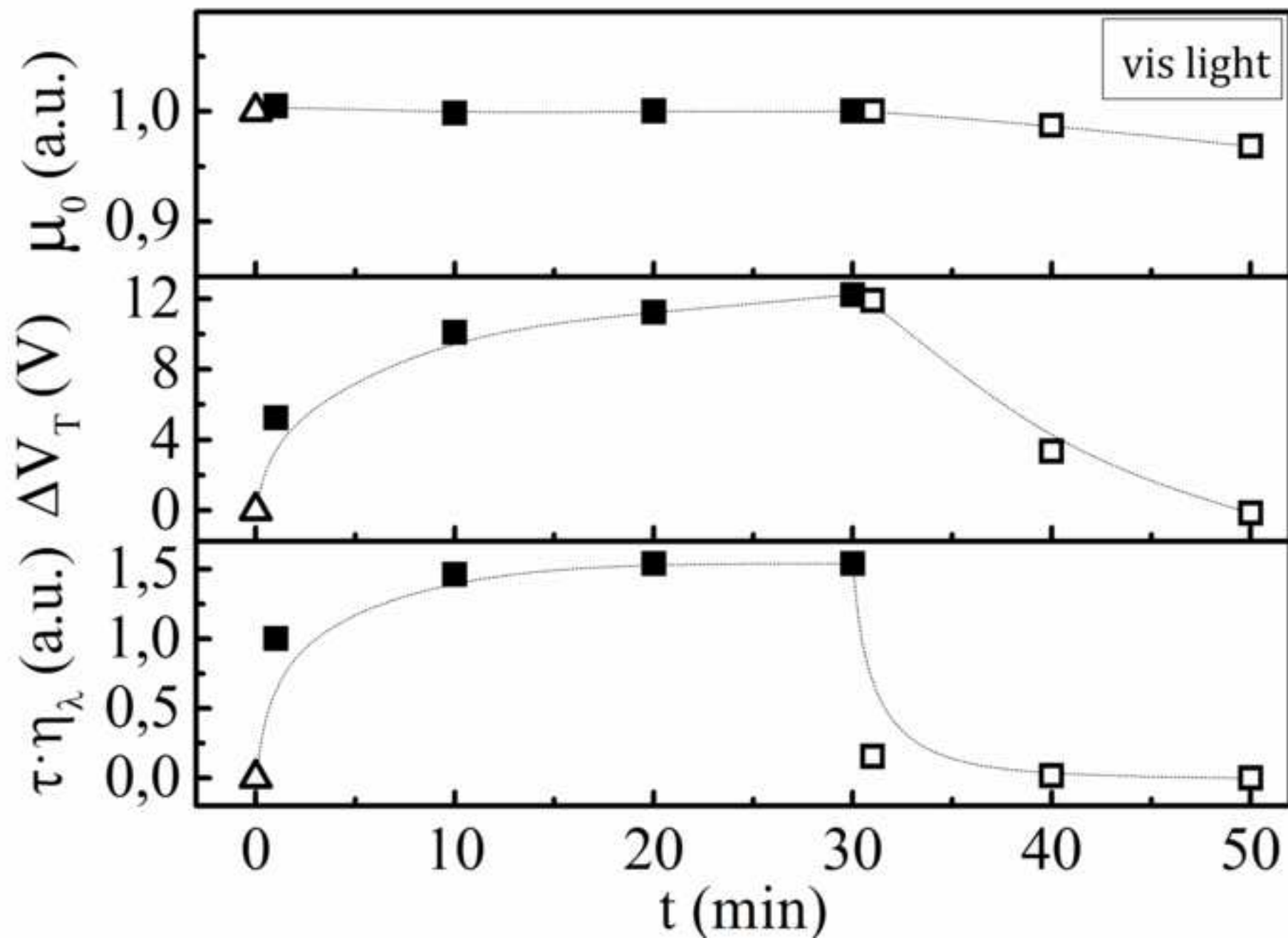


Figure11
[Click here to download high resolution image](#)

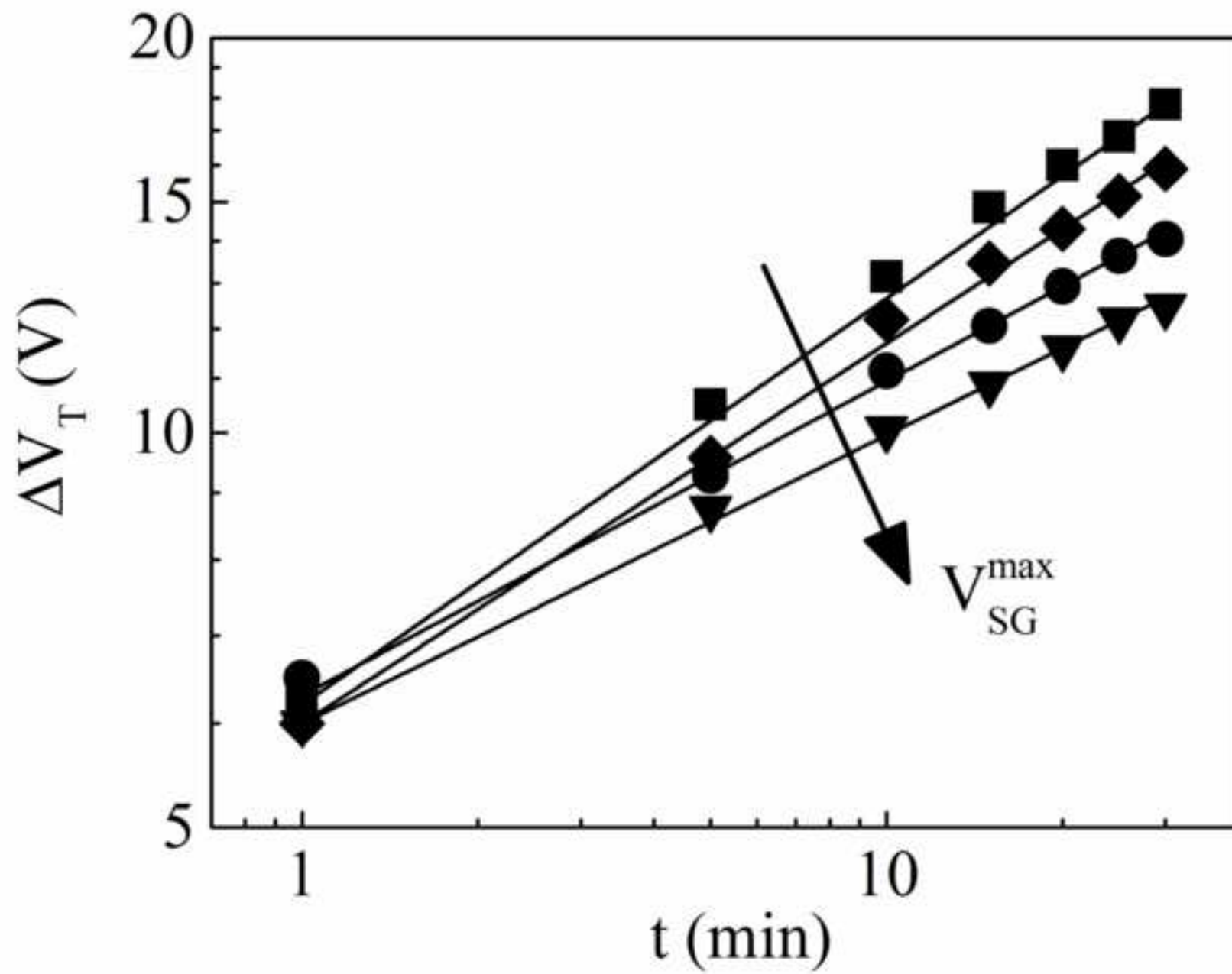


Figure12
[Click here to download high resolution image](#)

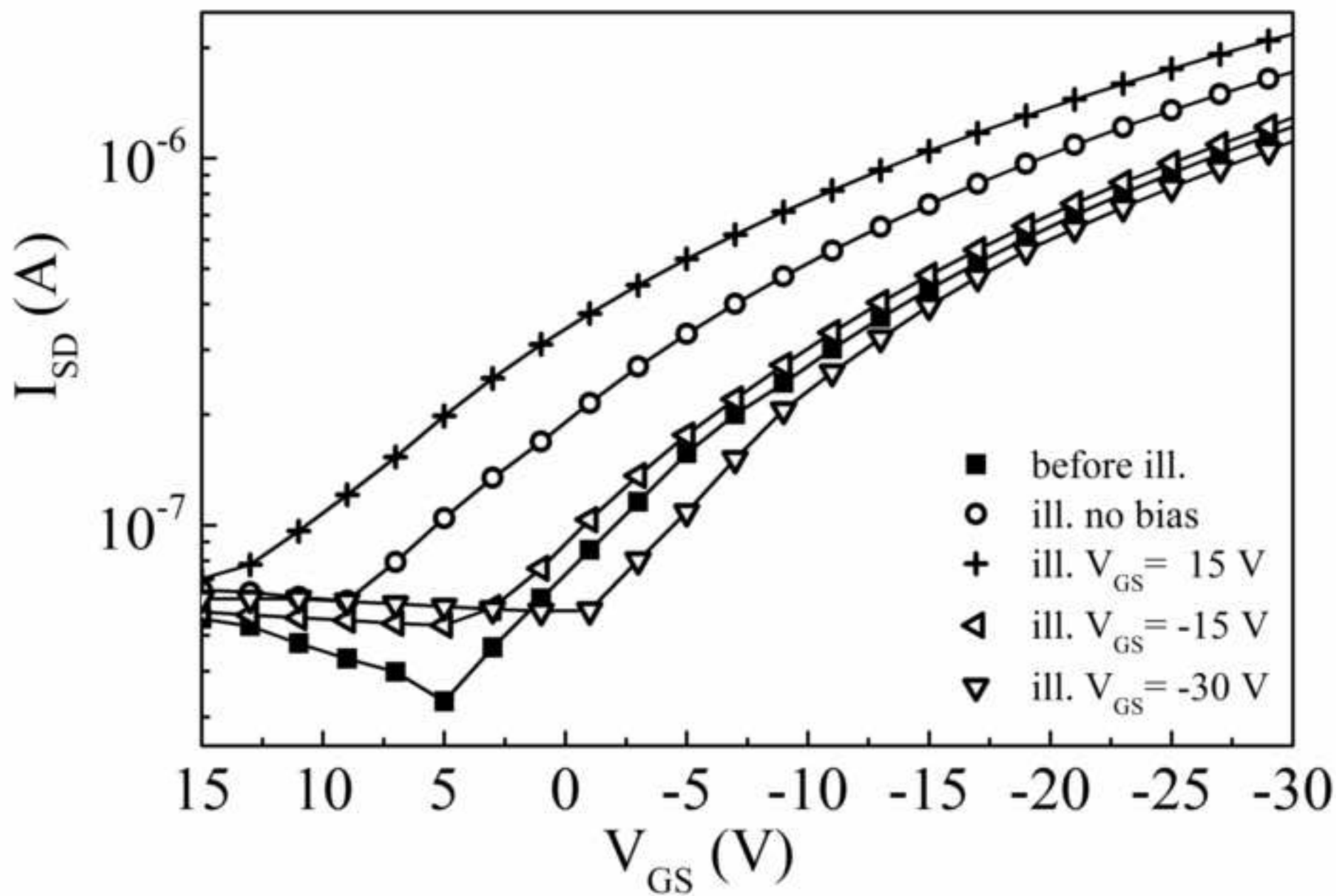


Figure13

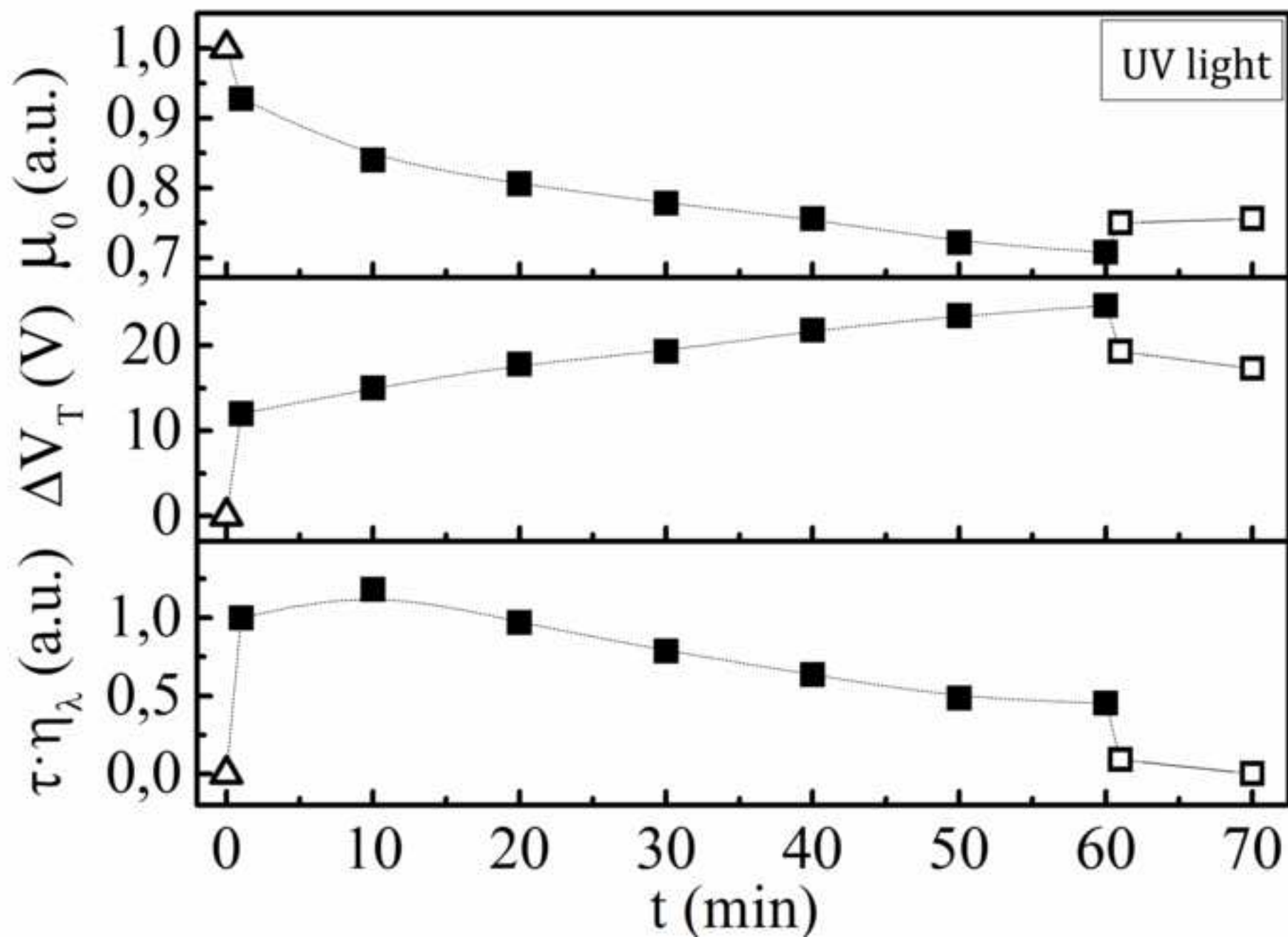
[Click here to download high resolution image](#)

Figure14

[Click here to download high resolution image](#)

